

Novel monoclonal antibody against integrin $\alpha 3$ shows therapeutic potential for ovarian cancer

Feng-Yi Ke^{1,2} | Wan-Yu Chen¹ | Ming-Chieh Lin³ | Yu-Chyi Hwang¹ |
Kuan-Ting Kuo^{2,3,4}  | Han-Chung Wu^{1,2} 

¹Institute of Cellular and Organismic Biology, Academia Sinica, Taipei, Taiwan

²Graduate Institute of Pathology, College of Medicine, National Taiwan University, Taipei, Taiwan

³Department of Pathology, National Taiwan University Hospital, Taipei, Taiwan

⁴Department of Pathology and Laboratory Medicine, National Taiwan University Hospital Hsin-Chu Biomedical Park Branch, Hsinchu County, Taiwan

Correspondence

Kuan-Ting Kuo, Department of Pathology, National Taiwan University Hospital, No. 7, Chung-Shan South Road, Taipei 10002, Taiwan.
Email: pathologykimo@gmail.com

Han-Chung Wu, Institute of Cellular and Organismic Biology, Academia Sinica, No. 128, Academia Road, Section 2, Nangang, Taipei 11529, Taiwan
Email: hcw0928@gate.sinica.edu.tw

Funding information

National Taiwan University, Grant/Award Number: NTU-CDP-103R7837; Program for Translational Innovation of Biopharmaceutical Development - Technology Supporting Platform Axis, Grant/Award Number: 107-0210-01-19-04; Ministry of Science and Technology, Grant/Award Number: MOST-108-2823-8-001-001 and MOST-108-3114-Y-001-002; Academia Sinica, Grant/Award Number: AS-SUMMIT-108

Abstract

Ovarian cancer has a high recurrence rate after platinum-based chemotherapy. To improve the treatment of ovarian cancer and identify ovarian cancer-specific antibodies, we immunized mice with the human ovarian carcinoma cell line, SKOV-3, and generated hybridoma clones. Several rounds of screening yielded 30 monoclonal antibodies (mAbs) with no cross-reactivity to normal cells. Among these mAbs, OV-Ab 30-7 was found to target integrin $\alpha 3$ and upregulate p53 and p21, while stimulating the apoptosis of cancer cells. We further found that binding of integrin $\alpha 3$ by OV-Ab 30-7 impaired laminin-induced focal adhesion kinase phosphorylation. The mAb alone or in combination with carboplatin and paclitaxel inhibited tumor progression and prolonged survival of tumor-bearing mice. Moreover, immunohistochemical staining of ovarian patient specimens revealed higher levels of integrin $\alpha 3$ in cancer cells compared with normal cells. By querying online clinical databases, we found that elevated ITGA3 expression in ovarian cancer is associated with poor prognosis. Taken together, our data suggest that the novel mAb, OV-Ab 30-7, may be considered as a potential therapeutic for ovarian cancer.

KEYWORDS

cell apoptosis, focal adhesion kinase, integrin $\alpha 3$, laminin, monoclonal antibody, ovarian cancer

Abbreviations: APC, allophycocyanin; CBP, carboplatin; FAK, focal adhesion kinase; IHC, immunohistochemistry; ITGA3, integrin $\alpha 3$ mRNA; NM, normal mouse; NNM, nasal mucosal epithelia; OPD, O-phenylenediamine dihydrochloride; PARP, poly(ADP-ribose) polymerase; PE, phycoerythrin; PI, propidium iodide; PTX, paclitaxel; TCGA, The Cancer Genome Atlas.

This is an open access article under the terms of the Creative Commons Attribution-NonCommercial-NoDerivs License, which permits use and distribution in any medium, provided the original work is properly cited, the use is non-commercial and no modifications or adaptations are made.

© 2020 The Authors. *Cancer Science* published by John Wiley & Sons Australia, Ltd on behalf of Japanese Cancer Association

1 | INTRODUCTION

Ovarian cancer is the most lethal gynecological cancer in the world. According to global cancer statistics, 295 414 new cases of ovarian cancer were diagnosed and 184 799 women died of the disease in 2018.¹ The overall 5-y survival rate for women diagnosed with ovarian cancer is 47%, and for women diagnosed with late-stage disease, the 5-y survival rate is only 29%.² About 75% of patients are diagnosed at advanced stages due to a lack of symptoms at early stages and a lack of reliable biomarkers for cancer screening.³ Currently, 2 main therapeutic strategies are used as first-line treatments for advanced ovarian cancer. One is optimal cytoreductive surgery followed by combination platinum- and taxane-based chemotherapy, and the other is neoadjuvant chemotherapy prior to interval debulking surgery.⁴ Approximately 80% of patients respond to first-line chemotherapy, but more than 70% of patients with advanced disease suffer a recurrence within 5 y and develop drug resistance.⁵⁻⁷

To improve patient survival and limit the damage to normal cells, targeted drugs, such as bevacizumab and poly (ADP-ribose) polymerase (PARP) inhibitors, have been developed.⁸⁻¹⁰ Bevacizumab is a humanized vascular endothelial growth factor A (VEGF-A)-targeting monoclonal antibody (mAb) that can inhibit tumor angiogenesis. The US FDA approved bevacizumab in 2018 for use in combination with carboplatin and paclitaxel, followed by bevacizumab monotherapy, to treat ovarian cancer.¹¹ Several clinical trials have shown that combined bevacizumab and chemotherapy can prolong progression-free survival from 2 to 4 mo; however no significant improvements have been reported for overall survival.¹²⁻¹⁴ Additionally, PARP inhibitors, such as fluzoparib, olaparib, and rucaparib, can inhibit tumor progression by disrupting DNA repair,^{15,16} and clinical studies have shown that these drugs have therapeutic potential for ovarian cancers with BRCA gene mutations.^{17,18} Although some studies have reported novel targeted therapies for ovarian cancer, there are still many more potentially useful surface molecules to be explored. Moreover, in spite of recent therapeutic advances, patient prognosis for ovarian cancer is still far from satisfactory.

Integrins are $\alpha\beta$ heterodimeric cell adhesion receptors that bind to extracellular matrix proteins and play important roles in cell adhesion, proliferation, and migration.¹⁹ Integrin $\alpha3$ and integrin $\beta1$ form a heterodimer that can bind to laminin²⁰⁻²² and is involved in the development of many organs, such as skin, kidney, lung, and brain.²³⁻²⁷ Several studies have identified integrin $\alpha3$ as a promising target molecule in brain and ovarian cancers, with potential utility in diagnosis and therapy.²⁸⁻³⁰ However, the cellular function of integrin $\alpha3$ in ovarian cancer remains largely unknown. One study found that reductions in integrin $\alpha3$ protein induced by WW domain-containing oxidoreductase gene led to diminished cancer cell tumorigenicity.³¹ Conversely, 2 other studies indicated that expression of integrin $\alpha3$ is inversely correlated with metastatic potential of human ovarian cancer.^{32,33} Therefore, further work will be required to understand the mechanistic role of integrin $\alpha3$ in ovarian cancer.

Because antibodies have high specificity for their target antigens, mAb therapeutics often cause fewer adverse effects in patients

compared with traditional chemotherapy.³⁴ Moreover, antibodies that specifically recognize ovarian cancer cells may be useful in diagnostic and/or therapeutic applications. In this work, we produced a mAb against ovarian cancer cells and investigated its therapeutic potential. Utilizing hybridoma technology, we generated mAbs from BALB/c mice after immunizing the animals with the ovarian cancer cell line, SKOV-3.

2 | MATERIALS AND METHODS

2.1 | Cell lines

The cell lines used in this study include mouse myeloma cell P3/NSI/1-Ag4-1 (NS-1), human ovarian carcinoma SKOV-3 (ATCC[®] HTB-77[™]) and ES-2 (ATCC[®] CRL-1978[™]), colorectal carcinoma HCT-116 (ATCC[®] CCL-247[™]), neuroepithelioma HTB-10 (ATCC[®] HTB-10[™]), hepatocellular carcinoma Mahlavu, lung carcinoma H460 (ATCC[®] HTB-177[™]), lung adenocarcinoma CL1-5, osteosarcoma U-2 OS (ATCC[®] HTB-96[™]), pancreatic adenocarcinoma MIA PaCa-2 (ATCC[®] CRL-1420[™]), breast adenocarcinoma MDA-MB-231 (ATCC[®] HTB-26[™]), oral carcinoma SAS, kidney carcinoma A-498 (ATCC[®] HTB-44[™]), human umbilical vein endothelial cells (HUVECs), foreskin fibroblast CCD-1112Sk (ATCC[®] CRL-2429[™]), and normal NNM cells. Primary NNM cultures were grown from biopsies of patients with nasal polyposis.³⁵ The use of NNM cultures was approved by the Human Subject Research Ethics Committee, Institutional Review Board, Academia Sinica (AS-IRB01-06008). NS-1 cells were purchased from Bioresource Collection and Research Center (Hsinchu, Taiwan). CL1-5 cells were acquired from Prof. Pan-Chyr Yang³⁶; Mahlavu cells were obtained courtesy of Dr. M. Hsiao (Genomic Research Center, Academia Sinica); SAS cells were obtained from the Japanese Collection of Research Bioresources (Tokyo, Japan); HUVECs were purchased from Lonza (Walkersville, MD, USA). Other cells were purchased from ATCC (Manassas, VA, USA). HUVEC were cultured in EBM-2 medium (Lonza), H460 in RPMI1640 (Thermo Fisher Scientific) medium, MDA-MB-231 in Leibovitz's L-15 medium and SAS in DMEM and Ham's F12 1:1 mix medium (Thermo Fisher Scientific). Other cell lines were cultured in DMEM. All culture media contained 10% fetal bovine serum (Thermo Fisher Scientific). The cell lines were all maintained at 37°C in humidified air with 5% CO₂.

2.2 | Generation of mAbs against ovarian cancer cells

The procedure to generate mAb against ovarian cancer cells has been described previously.^{37,38} In brief, female 6-wk-old BALB/cJ mice (Taiwan National University Animal Center, Taipei, Taiwan) were immunized by intraperitoneal (ip) injection of 1×10^7 live SKOV-3 cells without adjuvant. After the first immunization, 1×10^7 SKOV-3 cells mixed with 0.5 mL completed Freund's adjuvant was administered via ip injection. At 3 wk after the booster injection,

final boosters with 1×10^7 cells in PBS were administered via ip injection. On the fourth day after the final booster, splenocytes were harvested from the spleens of immunized mice and fused with NS-1 myeloma cells using 50% polyethylene glycol (Thermo). Fused cells were suspended in DMEM supplemented with hypoxanthine-aminopterin-thymidine (Sigma-Aldrich) and hybridoma cell growth supplement (MP Biomedicals), after which cells were seeded onto 96-well plates. The hybridomas that recognized SKOV-3, but not human foreskin fibroblast CCD-112Sk cells, were then clonally selected by limiting dilution, before being preserved in liquid nitrogen. Ascites were produced in pristane-primed BALB/cJ mice, and mAbs were purified using Protein G Sepharose 4 Fast Flow antibody purification resin (GE Healthcare Biosciences). The protocol for mouse experiments was approved by the Committee on the Ethics of Animal Experiments of Academia Sinica (AS IACUC: 15-09-853).

2.3 | Identification of mAb target protein

OV-Ab 30-7 was cross-linked with Protein G Sepharose (GE Healthcare Biosciences) using 60 mmol/L dimethyl pimelimidate. Total SKOV-3 cell lysates were applied to an OV-Ab 30-7-conjugated protein G affinity column. After washing, the proteins bound to OV-Ab 30-7 were eluted with elution buffer (0.2 mol/L glycine, pH 2.5, 150 mmol/L NaCl and 1% NP-40), and the eluates were neutralized with 1 mol/L Tris-HCl, pH 9.1.³⁹ The eluates were then separated by SDS-PAGE then stained using a SilverQuest™ Silver Staining Kit (Thermo Fisher Scientific). The band of interest was cut from the gel, reduced with 50 mmol/L dithioerythritol in 25 mmol/L ammonium bicarbonate (ABC) at pH 8.5 for 1 h at 37°C, and alkylated with 100 mmol/L iodoacetamide in ABC for 1 h at room temperature. After washing with 50% acetonitrile in ABC, the gel was soaked in 100% acetonitrile and incubated with 0.02 µg trypsin for 16 h at 37°C. The digested peptides were extracted with 50% acetonitrile in 5% TFA and concentrated using a Concentrator (Eppendorf). The sample was analyzed by LC-MS/MS sequencing, performed by the Core Facility for Proteomics and Structural Biology Research at Academia Sinica.

2.4 | Western blot analysis

Total cells were lysed using RIPA buffer (Cell Signaling Technology) containing protease inhibitor cocktail (Roche, Basel, Switzerland). Protein concentration was determined using a Pierce™ BCA Protein Assay Kit (Thermo Fisher Scientific). For non-reducing western blotting, protein was mixed with Native Sample Buffer (Bio-Rad) and, for reducing blots, protein was mixed with 4× Laemmli Sample Buffer containing 2-mercaptoethanol (Bio-Rad). Equal amounts of protein were separated by SDS-PAGE and transferred to polyvinylidene difluoride membranes (Merck Millipore). The membrane was blocked with 1% bovine serum albumin (BSA), and incubated with antibody

against PARP (sc-8007, Santa Cruz Biotechnology), FAK (#3285 Cell Signaling Technology), phospho-FAK (#8556, Cell Signaling Technology), integrin $\alpha 3$ (ab131055, Abcam), integrin $\beta 1$ (#9699, Cell Signaling Technology), p53 (#2524, Cell Signaling Technology) or p21 (#2947, Cell Signaling Technology) at a 1:1000 dilution overnight. The membrane was then incubated with HRP-conjugated secondary antibodies (Jackson ImmunoResearch, West Grove, PA, USA) for 1 h at room temperature, and signal was detected using an ECL kit (Merck).

2.5 | Flow cytometry

To determine whether the mAbs specifically bind SKOV-3 cells, SKOV-3, and CCD-112Sk cells were cultured overnight and then suspended using trypsin. Total cells (2×10^5) were transferred to 96-well shril-base plates and washed with FACS buffer (PBS containing 1% fetal bovine serum). After centrifugation (300 g at 4°C), the FACS buffer was carefully removed and cells were incubated with the hybridoma supernatant, or 1 µg/mL purified mAb or control antibody for 1 h at 4°C. Cells were then washed twice with FACS buffer and incubated with 100 µL phycoerythrin (PE)-labeled goat anti-mouse IgG (1/250 dilution) (Jackson ImmunoResearch) for 30 min at 4°C. Next, cells were washed twice with FACS buffer and suspended in 400 µL FACS buffer. Fluorescence signals were measured on a FACScan instrument (BD FACSCanto™ II, BD Biosciences, San Jose, CA, USA).

2.6 | Cellular ELISA

For hybridoma screening, 1×10^4 SKOV-3 or CCD-112Sk cells were plated into each well of 96-well polystyrene plates and, after an overnight incubation, cells were fixed with 2% paraformaldehyde for 20 min. The solution was removed and cells were washed with PBS twice, then blocked with 1% BSA in PBS for 4 h at 4°C. The hybridoma supernatants were diluted 2-fold with 1% BSA, and then incubated for 1 h at room temperature before incubation with HRP-conjugated goat anti-mouse IgG (Jackson ImmunoResearch) for 1 h. Plates were washed, and *o*-phenylenediamine dihydrochloride (Thermo Fisher Scientific) was used as a substrate; reactions were incubated for 7 min and stopped by the addition of 3 N HCl. Absorbance at 490 nm was measured on a microplate reader (Molecular Devices).

2.7 | Immunoprecipitation assay

SKOV-3 cell lysates and recombinant integrin $\alpha 3$ (#TP320975, OriGene, Rockville, MD, USA) or integrin $\beta 1$ (#H00003688-P01, Abnova, Taipei, Taiwan) were applied to OV-Ab 30-7 or NM IgG-coupled Protein G Sepharose (GE Healthcare Biosciences, Boston) for 1 h. Then the beads were washed 4 times with PBS containing

1% Tween-20. Proteins were eluted from the Protein G Sepharose with 2-mercaptoethanol and subsequently separated by SDS-PAGE for Western blotting. NM IgG-coupled Protein G Sepharose served as a negative control.

2.8 | Apoptosis assay

For apoptosis screening, cells were seeded and treated with hybridoma supernatant or antibodies for 6 h. Then cells were trypsinized and stained with FITC-annexin-V antibody and PI (BD Biosciences) in 200 μ L reaction buffer for 20 min at room temperature. The samples were analyzed by FACScan (BD FACSCanto™ II, BD Biosciences). Cells positive for FITC or both PI and FITC were counted as apoptotic, and those positive for PI only were considered necrotic cells.

2.9 | Sphere-forming assay

In total, 1×10^4 SKOV-3 and 2×10^3 ES-2 suspended single cells were seeded into an ultra-low attachment dish (Corning). Cells were cultured in serum-free DMEM-F12 with 10 ng/mL basic fibroblast growth factor (bFGF), 20 ng/mL epidermal growth factor (EGF) and B-27 Supplement (Thermo Fisher Scientific). After 10 d, spheres were photographed and lysed for western blotting.

2.10 | Immunofluorescence staining

Cells were seeded on cover slips and fixed with 2% paraformaldehyde for 20 min. After washing, cells were blocked with PBS containing 1% BSA for 30 min. Blocked cells were then incubated at room temperature with purified mAbs (2 μ g/mL) or NM IgG (2 μ g/mL), in 1% BSA. After 1 h incubation, cells were washed and incubated with Alexa Fluor 488 goat-anti-mouse antibodies. Nuclei were counterstained with 4',6-diamidino-2-phenylindole (DAPI; 1:10 000) (Thermo Fisher Scientific).

2.11 | Active caspase staining

SKOV-3 and SKOV-3 ITGA3-knockdown cells were treated with OV-Ab 30-7 (20, 2, 0.2 μ g/mL) or NM IgG (20 μ g/mL) for 6 h, and analyzed according to the manufacturer's instructions for the CaspGLOW™ fluorescein active caspase-3, 8, and 9 staining kit (Thermo Fisher Scientific). In brief, cells were harvested and incubated with FITC-conjugated caspase-3, 8, or 9 specific inhibitors for 1 h. After washing, cells were stained with APC-annexin-V (BD Biosciences) and PI. Finally, the cells were analyzed by flow cytometry (BD FACSCanto™ II, BD Biosciences). Cells negative for PI staining were analyzed for APC-annexin-V and active caspase-FITC.

2.12 | Cell adhesion assay

SKOV-3 cells were detached by 10 mmol/L EDTA in serum-free DMEM medium. Detached cells were washed with DMEM containing 1% BSA to remove the EDTA (Merck), and then incubated with OV-Ab 30-7 for 20 min. After incubation, 6×10^3 cells were seeded onto laminin-coated 96-well plates, which had been prepared by incubation with laminin 10 μ g/mL (LN332, BioLamina, Sundbyberg, Sweden) overnight at 4°C. After 45 min, the non-adherent cells were removed by washing with PBS, and the adhered cells were quantified by the MTT (Merck) assay.

2.13 | Immunohistochemistry (IHC) staining

In total, 31 human ovarian cancer surgical specimens were obtained from the archives of the Department of Pathology, National Taiwan University Hospital. This study was approved by the National Taiwan University Hospital Research Ethics Committee. For IHC, 4 μ m paraffin-embedded sections were stained using the Super Sensitive™ IHC Detection System (BioGenex) according to the manufacturer's directions. Anti-integrin α 3 (MAB1952Z, Merck) and anti-laminin antibody (ab17107, Abcam) were diluted to 1:100 and incubated with tissue sections overnight. Samples with less than 1% positive cells were considered as negative staining. The intensity of staining in positive cases was graded as weak, moderate, or strong. Staining was evaluated by a pathologist, Dr. Kuo, K-T.

2.14 | Knockdown of ITGA3

Stable ITGA3-knockdown (clone: TRCN0000057714) or luciferase-knockdown control (clone: TRCN0000231719) SKOV-3 cells were generated by transduction of lentiviruses with short hairpin RNAs cloned into the pLKO.1 vector. RNAi reagents were obtained from the National RNAi Core Facility located at the Institute of Molecular Biology/Genomic Research Center, Academia Sinica, Taipei, Taiwan. The human shRNA library was TRC-Hs 1.0. Stable cells were selected with puromycin for 1 wk.

2.15 | In vitro migration assays

For the migration assay, 5×10^4 cells were suspended in serum-free DMEM and plated onto membranes (8- μ m pore size, Merck) that were coated with laminin (LN332, BioLamina). Medium containing 10% FBS was added to the lower chamber as a chemoattractant. Following incubation for 18 h at 37°C, non-invading cells on the upper surface of the filter were removed with a cotton swab. The invading cells on the lower surface of the filter were fixed and stained with hematoxylin and eosin. The cell motility and invasiveness were determined by counting cells in 5 microscopic fields per well, and the extent of invasion was expressed as the average number of cells per field.

2.16 | Antitumor efficacy

The procedure to evaluate antitumor efficacy *in vivo* was modified from a previous study.⁴⁰ In brief, NOD/SCID mice were obtained from the Jackson Laboratory and were bred in the core facility of the Institute of Cellular and Organismic Biology at Academia Sinica. Female NOD.CB17-Prkdcscid/JNarl mice (4–6 wk old), were injected ip with 1×10^7 SKOV-3 cells suspended in 100 μ L DMEM (serum free). To investigate the therapeutic efficacy of OV-Ab 30-7, 20 mg/kg OV-Ab 30-7 or NM IgG was simultaneously injected with the tumor cells. Mouse survival was recorded twice a week.

For the xenograft mouse model, 5×10^6 SKOV-3 cells were injected subcutaneously in the dorsal right flank. When the tumor reached 100 mm³, the mice were randomly divided into 2 treatment groups (each $n = 8$): NM IgG (20 mg/kg), OV-Ab 30-7 (20 mg/kg). The OV-Ab 30-7 and control IgG were injected twice weekly through the tail vein. Tumor diameters were measured using calipers at 4-d intervals, and tumor volumes were calculated using the formula, width² \times length \times 0.52.

For combination therapy, tumor-bearing mice were randomly sorted into 6 groups (each group, $n = 6$): Group A, Vehicle control; B, PTX (5 mg/kg); C, CBP (30 mg/kg); D, CBP (15 mg/kg) + PTX (2.5 mg/kg); E, OV-Ab 30-7 (20 mg/kg); and F, CBP (15 mg/kg) + PTX (2.5 mg/kg) + OV-Ab 30-7 (20 mg/kg). Treatments were initiated 1 h after inoculation with tumor cells. Drug and antibodies were administered by ip injection twice a week for 4 wk consecutively. Mice survival rates were recorded twice a week.

For the *in vivo* bioluminescence assay, SKOV-3 and ES-2 cells were infected with Lenti-luc virus (lentivirus containing the luciferase gene). After puromycin selection, 1×10^7 SKOV-3-Luc or 2×10^6 ES2-Luc cells were ip injected into 4- to 6-wk-old female NOD/SCID mice. At 2 d after inoculation of tumor cells, 150 mg/kg D-luciferin (Goldbio) was injected ip, and bioluminescence was quantified by an Xtreme II (Bruker). Mice were then separated into 3 groups: Group A, Vehicle control; B, CBP (15 mg/kg) + PTX (2.5 mg/kg); and C, CBP (15 mg/kg) + PTX (2.5 mg/kg) + OV-Ab 30-7 (20 mg/kg). Drug and antibody were administered by ip injection twice a week for 4 wk consecutively. Tumor progression was monitored by bioluminescence quantification. Mouse body weight and survival rate were recorded. Animal care was carried out in accordance with the guidelines of Academia Sinica, Taiwan. The protocol was approved by the Committee on the Ethics of Animal Experiments at Academia Sinica. PTX was provided by ScinoPharm Taiwan, Ltd. (SPF2039, Tainan, Taiwan) and CBP were purchased from Abcam (ab120828).

2.17 | Statistical analysis

The binding, apoptosis, caspase activities, and migration assays were analyzed using a two-tailed unpaired Student *t* test. *P*-values below .05 were considered significant for all analyses. Values were expressed as means \pm SD unless otherwise specified. All data were

derived from at least 3 independent experiments. Survival analyses were performed using Kaplan-Meier survival curves, and significant differences between groups were tested using a log-rank test. Correlation coefficients were assayed by Spearman analysis. IHC staining for protein co-expression was analyzed by Pearson chi-squared test.

3 | RESULTS

3.1 | Generation and characterization of mAbs against ovarian cancer cells

Compared with other epithelial ovarian cancer subtypes, clear cell ovarian carcinoma is more frequently aggressive and drug resistant.⁴¹ Therefore, we utilized SKOV-3 cells to develop a new therapeutic mAb for clear cell carcinoma. SKOV-3 cells are a well characterized cell line that is frequently used for ovarian cancer antigen studies.^{42–44} We injected SKOV-3 cells into the peritoneal cavity of BALB/cJ mice 3 times at 3-wk intervals to serve as an immunogen for antibody production. More than 2800 hybridoma clones against ovarian cancer cells were generated by this procedure. After characterizing the clones by both cellular ELISA and flow cytometry, we selected 30 hybridoma clones with high reactivity and specificity against SKOV-3 cells and no cross-reactivity with CCD-1112Sk cells (Supporting information Figure S1A,B). To identify mAbs from each selected clone, single hybridoma cells were seeded into wells of a 96-well plate by serial dilution. The mAbs were tested by cellular ELISA (Figure S1C) to confirm their binding affinity for SKOV-3 cells. All 30 mAbs showed high binding affinity for SKOV-3 cells without cross-reactivity to CCD-1112Sk cells. We also tested binding of the mAbs to other cancer cell lines, including ES-2, HCT-116, HTB-10, Mahlavu, H460, MDA-MB-231, MIA PaCa-2, U-2OS, CL1-5, SAS, and A-498. Additionally, binding to non-cancerous cells, NNM, CCD-1112Sk, and HUVECs, was also tested. Most of the mAbs showed low affinity to normal cells (Figure S2A).

To identify the target proteins of these mAbs, SKOV-3 whole-cell lysates were used for western blotting under denaturing conditions. OV-Ab 1-21, OV-Ab 2-1, OV-Ab 4-2, OV-Ab 5-3, OV-Ab 8-11, OV-Ab 9-2, OV-Ab 10-6, OV-Ab 11-1, OV-Ab 12-1, and OV-Ab 13-2 all recognized a protein of 38 kDa. Three other mAbs, OV-Ab 15-23, OV-Ab 20-4, and OV-Ab 22-13, recognized 2 proteins with molecular weights of 170 and 120 kDa on the reducing gel. OV-Ab 7-12 recognized a protein with a molecular weight of approximately 170 kDa on the reducing gel. The remaining mAbs did not obviously recognize any particular protein in either reducing or non-reducing western blots (Figure S2B). Additionally, only OV-Ab 15-23 weakly recognized proteins with molecular weights of 170 and 120 kDa in CCD-1112Sk cell lysates. The rest of the mAbs produced either low or undetectable bioluminescence signals when incubated with CCD-1112Sk cell lysates, as compared with the signals from SKOV-3 cells lysates (Figure S2C). Immunofluorescence staining revealed that OV-Ab 3-5, OV-Ab 7-12, OV-Ab 10-6, OV-Ab 13-2,

OV-Ab 25-3, and OV-Ab 30-7 exhibited extremely high cell-surface binding to SKOV-3 cells, without any detectable binding to NNM cells (Figure S2D). We then used the bicinchoninic acid method to standardize the concentrations of these 6 mAbs and determined the relative binding affinity to SKOV-3 cells with cellular ELISA and flow cytometry. We found that among these 6 mAbs, OV-Ab 30-7 had the best affinity for SKOV-3 cells (Figure S3A,B).

To evaluate the ability of mAbs to induce cancer cell apoptosis, we incubated SKOV-3 cells with each mAb for 6 h and then stained the cells with PI and FITC-labeled annexin-V. OV-Ab 6-3, OV-Ab 13-2, OV-Ab 16-13, OV-Ab 19-13, OV-Ab 25-3, and OV-Ab 30-7 all induced apoptosis in more than 20% of the cell population (Figure S1D). Importantly, we found that, in addition to showing the highest affinity to SKOV-3 cells, OV-Ab 30-7 also produced the highest percentage of apoptotic cells (Figure S1D and Table S1).

3.2 | Identification of integrin $\alpha 3$ as the target molecule for OV-Ab 30-7

To identify which surface protein of the SKOV-3 cells was recognized by OV-Ab 30-7, we cross-linked protein G beads with the mAb and immunoprecipitated SKOV-3 total cell lysates. We identified a 120 kDa protein as a target by silver staining the immunoprecipitate on an SDS-PAGE gel (Figure 1A). Subsequently, the bands were excised from the gel and analyzed by mass spectrometry, revealing 31% sequence coverage of integrin $\alpha 3$ (Figure 1B) and 29% coverage of integrin $\beta 1$ (Figure S5C). As OV-Ab 30-7 could pull down both

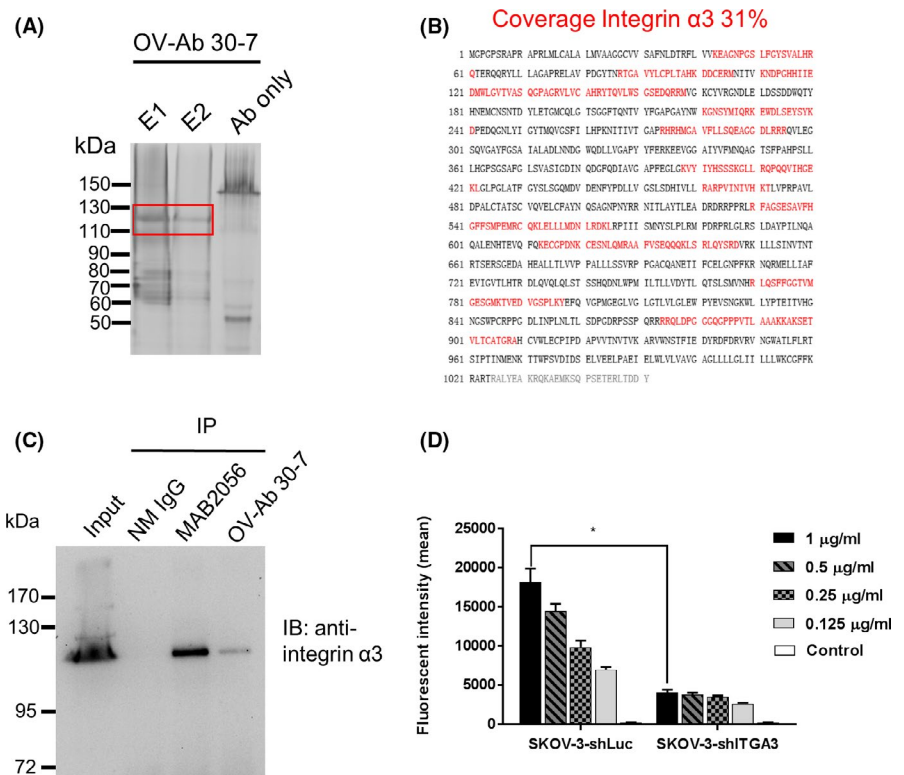
integrin $\alpha 3$ and integrin $\beta 1$ proteins (Figures 1C and S5A), we then used the recombinant proteins for immunoprecipitation to determine which one was the antigen. Only integrin $\alpha 3$ was precipitated by OV-Ab 30-7 (Figure S5B). Moreover, small hairpin RNA (shRNA)-mediated knockdown of integrin $\alpha 3$ mRNA (shITGA3) in SKOV-3 cells drastically reduced OV-Ab 30-7 binding affinity (Figure 1D) and OV-Ab 30-7-induced cell apoptosis (Figure 2A) compared with cells with control knockdown of luciferase (shLuc). Efficient integrin $\alpha 3$ knockdown was validated by western blotting (Figure S5D). Together, these results showed that OV-Ab 30-7 specifically recognizes integrin $\alpha 3$.

3.3 | OV-Ab 30-7 induces SKOV-3 cell apoptosis through integrin $\alpha 3$

No other antibodies have been previously reported to directly induce apoptosis in ovarian cancer cells. Thus, our finding that OV-Ab 30-7 dose-dependently induced apoptosis in SKOV-3 cells (derived from ascites of a patient with ovarian serous cystadenocarcinoma) and ES-2 cells (derived from a poorly differentiated ovarian clear cell carcinoma tumor) with no effect on ITGA3-knockdown SKOV-3 cells or normal epithelial NNM cells (Figure 2A) warranted further exploration.

We treated SKOV-3 cells and ITGA3-knockdown cells with OV-Ab 30-7 for 6 h and then probed caspase 3, caspase 8, or caspase 9 activities by flow cytometry. The activation levels of all 3 caspases were dose-dependently enhanced by OV-Ab 30-7 antibody treatment, but the levels were not significantly affected

FIGURE 1 Identification of integrin $\alpha 3$ as the target antigen of OV-Ab 30-7. A, Silver staining of proteins eluted from OV-Ab 30-7-conjugated protein G affinity column. E1, E2: elution supernatants from protein G-OV-Ab 30-7 affinity column. Ab only: 5 μ g/mL OV-Ab 30-7. B, Peptide sequences of the target protein were deduced from MS/MS analysis. Identified peptides are shown in red. C, SKOV-3 cell lysates were immunoprecipitated with normal mouse (NM) IgG, MAB2056 commercial anti-integrin $\alpha 3$ antibody, or OV-Ab 30-7 antibody. Western blotting was performed with rabbit anti-integrin $\alpha 3$ antibody. D, Flow cytometric analysis of OV-Ab 30-7 binding to ITGA3 and luciferase knockdown SKOV-3 cells. Cells (2×10^5 per condition) were incubated with different concentrations of OV-Ab 30-7 and detected with PE-conjugated anti-mouse IgG. * $P < .05$



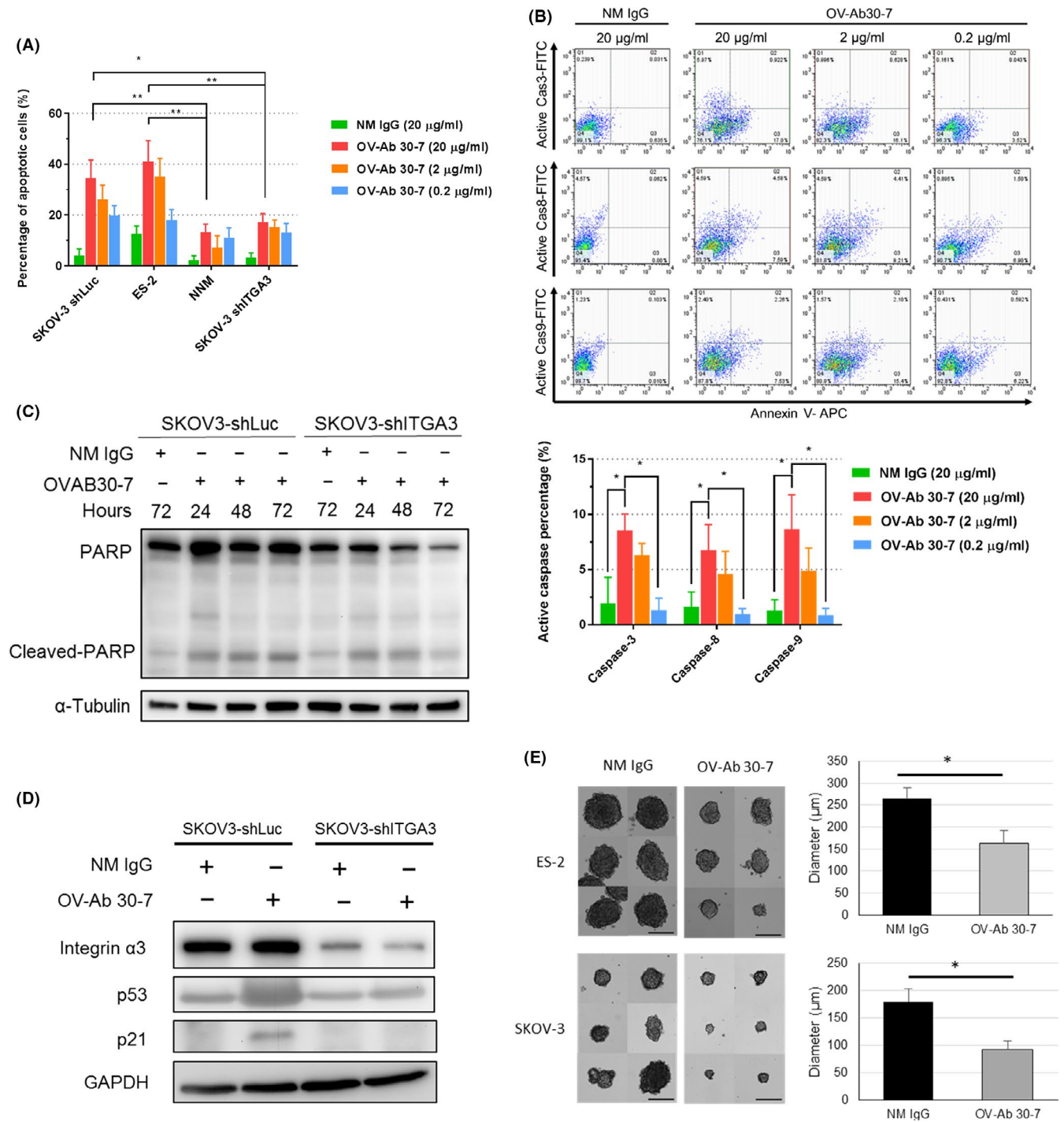


FIGURE 2 OV-Ab 30-7 induces apoptosis, p53 upregulation, caspase activation, and PARP cleavage in SKOV-3 cells. **A**, Apoptosis of SKOV3-shLuc, ES-2, NNM, and SKOV-3 integrin α 3-knockdown cells. FITC-annexin-V and PI staining were used to detect apoptosis after incubation with 0.2, 2, or 20 μ g of OV-Ab 30-7 or NM IgG for 6 h. * $P < .05$, ** $P < .01$. **B**, Flow cytometry analysis of caspase-3, 8, and 9 activation in SKOV-3 cells. Cells were treated with NM IgG or OV-Ab 30-7 for 6 h at the indicated concentrations. Representative histograms are shown, with quantitative results below. **C**, Western blot analysis of cleaved PARP in SKOV-3 cells. Cells were treated with OV-Ab 30-7 or NM IgG (40 μ g/mL) for 24, 48, and 72 h. **D**, Western blot analysis of p53 and p21. Cells were treated with OV-Ab 30-7 or NM IgG for 30 min. **E**, Representative images of ES-2 (upper) and SKOV-3 (lower) cells treated with 20 μ g/mL OV-Ab 30-7 or NM IgG. Quantification of the spheroid diameters is shown to the right. Scale bar, 200 μ m

in ITGA3-knockdown cells at any dose (Figures 2B and S6A). Furthermore, we treated SKOV-3 cells with OV-Ab 30-7 for 24, 48, or 72 h and then assessed PARP cleavage by western blot. OV-Ab

30-7 treatment led to an increased level of cleaved PARP protein compared with NM IgG. Moreover, OV-Ab 30-7-induced PARP cleavage was attenuated by knockdown of ITGA3 (Figure 2C). We

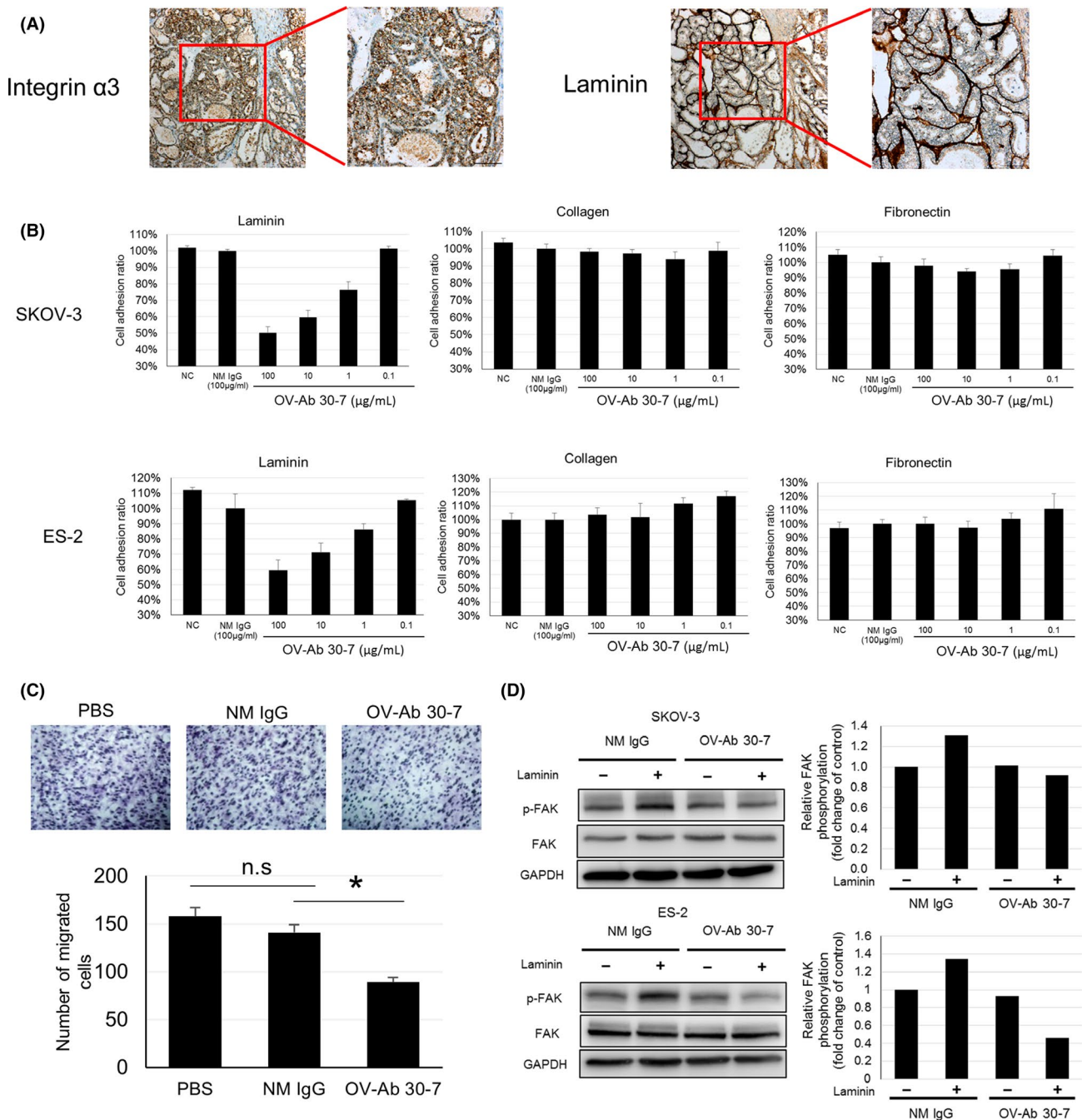
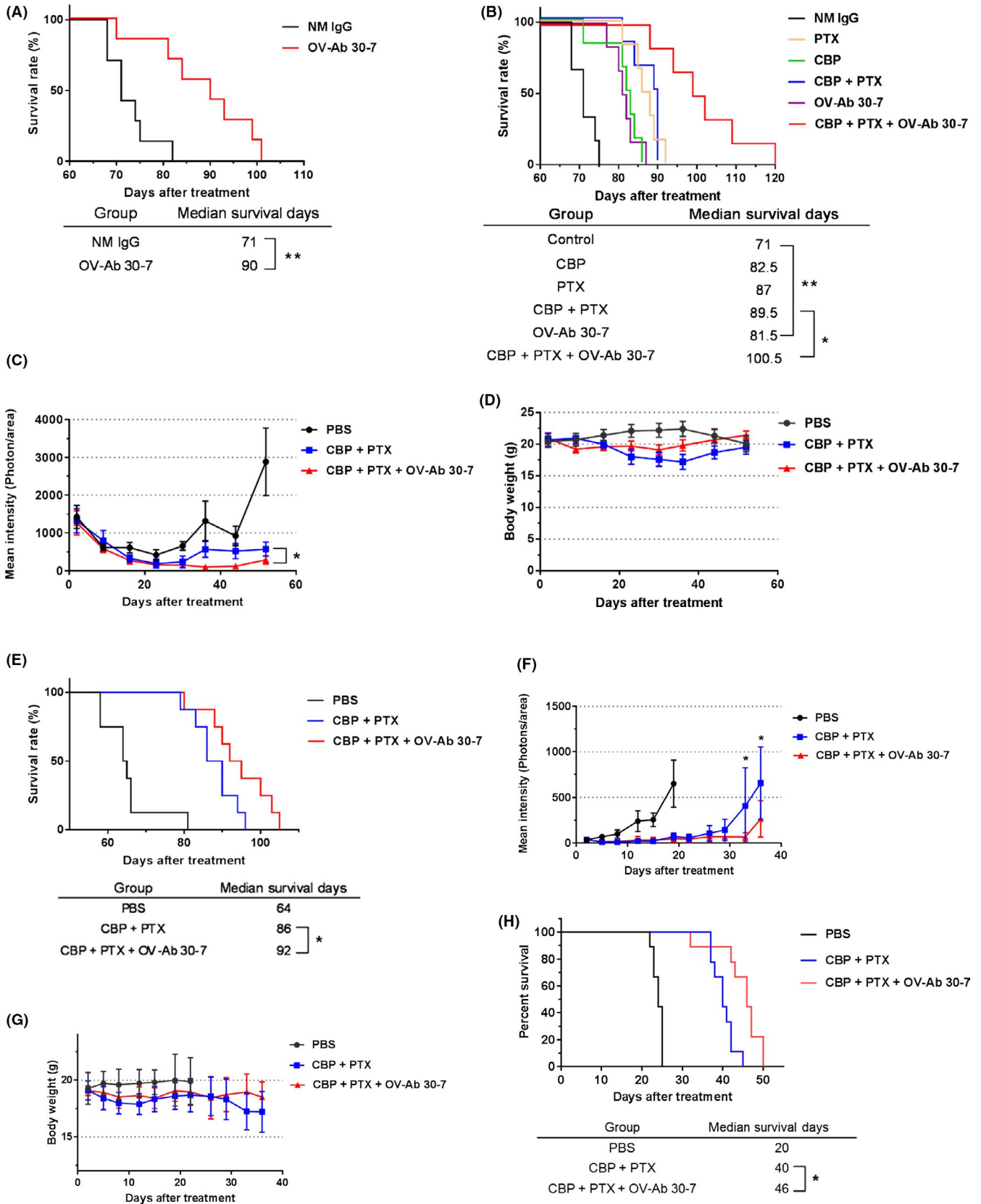


FIGURE 3 Integrin $\alpha 3$ is co-expressed with laminin and OV-Ab 30-7 can block laminin-integrin signaling. A, IHC staining of integrin $\alpha 3$ and laminin- $\alpha 5$ in ovarian cancer tissue reveals co-expression of the proteins. Scale bars, 100 μm ($\times 200$). B, Cell adhesion assay. SKOV-3 and ES-2 cells were seeded on laminin, fibronectin or collagen-coated plates for 45 min. After washing, adherent cells were quantified relative to control. C, Transwell migration assay. SKOV-3 cells were treated with PBS, NM IgG, or OV-Ab 30-7 (20 $\mu\text{g}/\text{mL}$), then seeded on laminin-coated wells for 8 h. D, SKOV-3 and ES-2 cells were pre-incubated with OV-Ab 30-7, NM IgG for 15 min at 37°C, then seeded on plates with or without laminin coating for 30 min. Western blot analysis of the indicated proteins was performed. Right panel shows the quantification of phosphorylated FAK signal from western blots

FIGURE 4 OV-Ab 30-7 inhibits tumor growth in vivo. NOD/SCID mice were injected ip with 1×10^7 SKOV-3 cells (A) followed by treatment with 20 mg/kg OV-Ab 30-7 or NM IgG. OV-Ab 30-7-treated mice had prolonged survival compared with those treated with NM IgG (each group $n = 7$). B, At 1 h after tumor cell injection, mice were treated with NM IgG, PTX, CBP, OV-Ab 30-7, PTX + CBP, or PTX + CBP combined with OV-Ab 30-7 (each group $n = 6$). Kaplan-Meier survival curves were generated, and the median survival day is shown. C-E, Mice injected ip with 1×10^7 SKOV-3-Luc cells were treated with PBS, CBP + PTX, or CBP + PTX combined with OV-Ab 30-7. C, Tumor bioluminescence, D, body weight, and E, survival were monitored on the indicated days. Each group, $n = 8$. F-H, NOD/SCID mice injected ip with 2×10^6 ES2-Luc cells were treated with PBS, CBP + PTX, or CBP + PTX combined with OV-Ab 30-7. F, Tumor bioluminescence, G, body weight, and H, survival were monitored. Each group, $n = 9$ Error bars, SD. * $P < .05$, ** $P < .01$



also found that p53 and p21 were upregulated in SKOV-3 cells after OV-Ab 30-7 treatment, an effect that was also attenuated by knock-down of ITGA3 (Figure 2D). Collectively, these results suggested

that OV-Ab 30-7 induced ovarian cancer cell apoptosis by targeting integrin $\alpha 3$. We then sought to investigate whether OV-Ab 30-7 could induce cell apoptosis in breast and pancreatic cancer. We

FIGURE 5 Integrin $\alpha 3$ and laminin expression in ovarian cancer correlate with poor prognosis. A, IHC staining of integrin $\alpha 3$ in ovarian cancer and tumor-adjacent normal ovary tissue. B, Positive and negative integrin $\alpha 3$ IHC staining in the different types of ovarian cancer. C, Overall survival of ovarian cancer patients from the TCGA database stratified by expression of ITGA3, ITGB1, or both. Gene expression was determined by RNA sequencing and reported as median number Fragment Per Kilobase of exon per Million (FPKM) reads. The cut-off value for ITGA3 was 35.34, and for ITGB1, it was 44.09 FPKM. D, In total, 31 clinical ovarian cancer specimens were analyzed by IHC for laminin- $\alpha 5$ and integrin $\alpha 3$. Representative images of weak, moderate, and strong staining are shown. The number of cases with each staining intensity is indicated in the table below ($P < .01$). E, Relationships between ITGA3 and laminin-related gene expression in patients from the TCGA database. Data were visualized by cBioPortal (<https://www.cbioportal.org/>) and evaluated with Pearson's correlation analysis. F, Kaplan-Meier survival curves of ovarian cancer patients stratified by LAMA3, LAMB3, and LAMC2 expression. G, Kaplan-Meier survival curves for ovarian cancer patients stratified by ITGA3 expression combined with laminin-related gene (LAMA3, LAMB3, LAMC2) expression

found that OV-Ab 30-7 could induce apoptosis in MDA-MB-234 and BxPC3 cells, which have a high binding affinity for the antibody. In contrast, cells with low binding affinity, such as AsPC1, SU.86.86, ZR75 and SKBR3, did not undergo apoptosis after OV-Ab 30-7 treatment (Figure S7A, B).

As integrin expression is known to regulate formation of spheroids by ovarian cancer cells,^{45,46} we next examined whether OV-Ab 30-7 could affect spheroid formation in 3D cultures. The results showed that spheroid diameter was significantly smaller when cells were treated with OV-Ab 30-7 compared with control antibody NM IgG (Figure 2E).

3.4 | OV-Ab 30-7 inhibits integrin $\alpha 3$ -laminin signaling in SKOV-3 cells

Laminin serves as the ligand for the integrin $\alpha 3\beta 1$ heterodimer.^{47,48} Using IHC staining, we found that integrin $\alpha 3$ and laminin were both expressed in ovarian tumor tissue (Figure 3A). We then examined whether OV-Ab 30-7 could block integrin $\alpha 3$ binding to major components of the extracellular matrix. Plates were pre-coated with laminin, collagen, or fibronectin. Then, cells were mixed with OV-Ab 30-7 or control Ab and seeded onto the pre-coated plates. OV-Ab 30-7 inhibited SKOV-3 and ES-2 cell adhesion to the laminin-coated plate in a dose-dependent manner, but cell binding was not inhibited in fibronectin or collagen-coated plates. (Figure 3B). Furthermore, we found that OV-Ab 30-7 inhibited SKOV-3 cell migration on a laminin-coated substrate (Figure 3C). Next, we probed the intracellular signaling pathways activated by integrin. We found that FAK proteins were phosphorylated when cells were seeded on a laminin-coated plate, and this effect was inhibited by OV-Ab 30-7 in both SKOV-3 and ES-2 cells (Figure 3D).

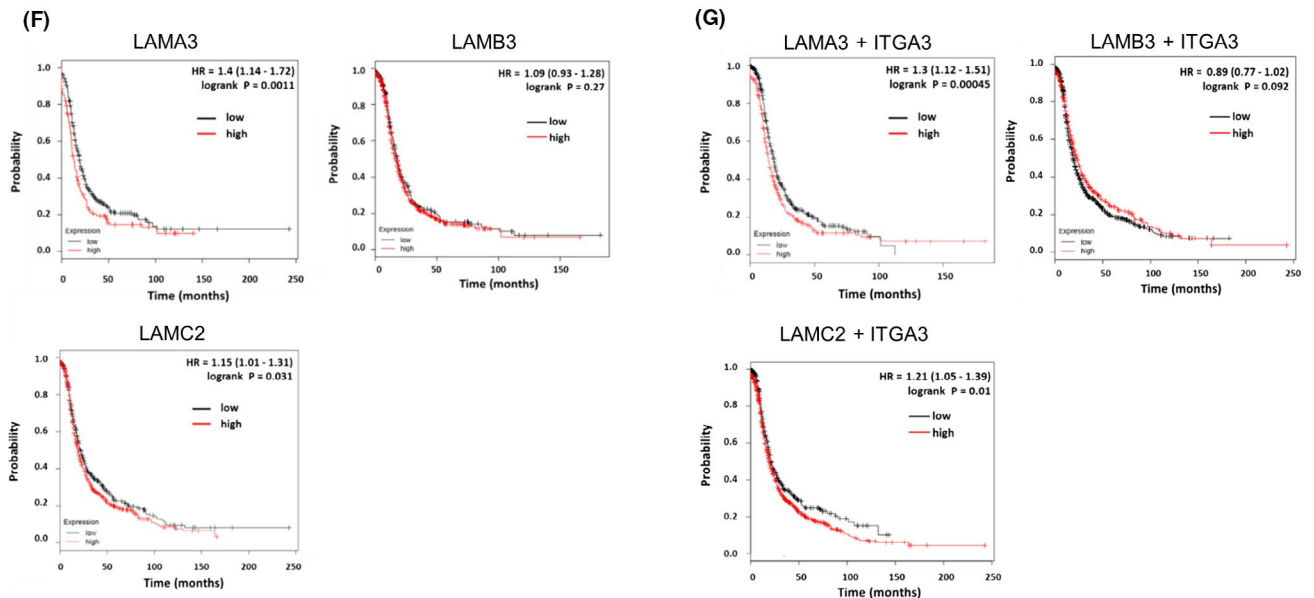
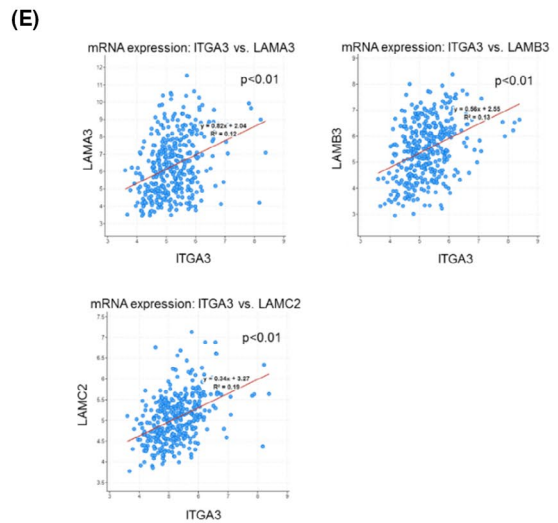
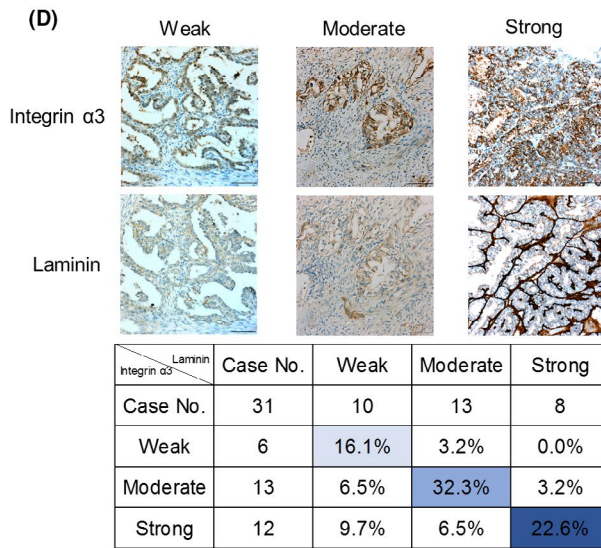
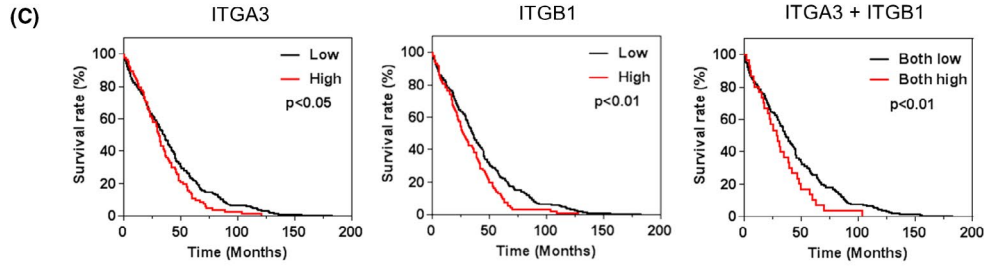
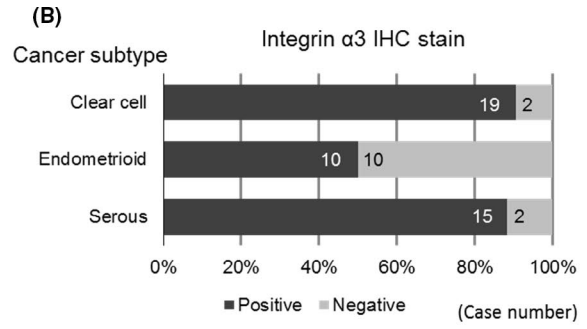
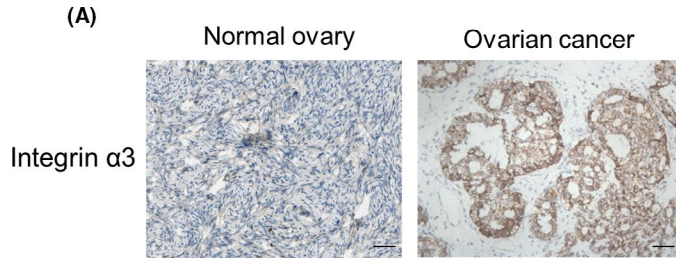
3.5 | OV-Ab 30-7 improves ovarian cancer survival in vivo

To evaluate the therapeutic potential of OV-Ab 30-7 for primary ovarian cancer tumors, we treated a xenograft mouse model with OV-Ab 30-7 or vehicle control. However, OV-Ab 30-7 treatment did not significantly inhibit tumor growth compared with the vehicle control (Figure S8A, B). Adverse effects of OV-Ab 30-7 were then

evaluated in tumor-bearing mice treated with twice-a-week injections of OV-Ab 30-7 for 4 wk consecutively at a dose of 20 mg/kg per injection. The vital organs, including the heart, kidney, and lung, exhibited no significant pathological changes (Figure S8C). To further probe metastatic disease, we co-injected SKOV-3 cells with OV-Ab 30-7 or NM IgG into the peritoneal cavity of SCID mice. When SKOV-3 cells were co-injected with OV-Ab 30-7 (Figure 4A), the median survival of mice was longer than that of the group receiving NM IgG. Next, to examine whether the OV-Ab 30-7 has the ability to improve the currently preferred treatment for ovarian cancer, PTX, CBP, and OV-Ab 30-7 were co-treated as a combination therapy in vivo. At 1 h after SKOV-3 cells were injected into the peritoneal cavity, mice were treated with PTX, CBP, and OV-Ab 30-7 alone or in combination. Again, tumor-bearing mice treated with OV-Ab 30-7 exhibited longer median overall survival compared with NM IgG-treated animals. Moreover, combining OV-Ab 30-7 treatment with PTX and CBP was significantly more effective than combined PTX and CBP treatment (Figure 4B). To examine tumor growth in the mice, we injected SKOV-3-Luc or ES2-Luc cells, which stably express firefly luciferase, into the peritoneal cavity. To mimic clinical treatment for metastatic disease, 2 d after tumor cell injection, mice were treated with PTX and CBP or a combination of OV-Ab 30-7 with both chemotherapeutics (Figure 4C-H). Tumor growth was monitored non-invasively using bioluminescence imaging. PTX and CBP combined with OV-Ab 30-7 showed better tumor growth inhibition and prolonged survival without affecting body weight when compared with the PTX and CBP combination (Figure 4C-H).

3.6 | Integrin $\alpha 3$ and laminin are overexpressed in ovarian tumors and Integrin $\alpha 3$ overexpression correlates with poor prognosis

IHC staining of integrin $\alpha 3$ in ovarian cancer and tumor-adjacent normal ovary tissues are shown in Figure 5A. Integrin $\alpha 3$ was found to be overexpressed in tumors compared with normal tissue. To examine the integrin $\alpha 3$ expression profile in ovarian cancer, we analyzed 3 different histological types of tissue by IHC staining and found that integrin $\alpha 3$ was most often highly expressed in clear cell (19/21, 90.47%) and serous type (15/17, 88.24%) ovarian cancers; only half of endometrioid type tissues (10/10, 50%) were considered to have high expression (Figure 5B). Furthermore, clinical data from



TCGA databases were analyzed, showing that patients had significantly better survival when tumors expressed low levels of *ITGA3*, *ITGB1*, or both ($P < .05$, Figure 5C). As histology type and tumor grade influence survival of ovarian cancer patients,⁴⁹ we used the Kaplan-Meier Plotter database (<http://kmpplot.com/analysis/index.php?p=service&cancer=ovar>) to analyze the association of prognosis and *ITGA3* expression according to histology type and tumor grade. The results showed that high expression of *ITGA3* correlated with poor survival in serous and endometrioid histology types (Figure S9A), and high expression also significantly correlated with poor survival in grade 3 serous type ovarian cancer. (Figure S9B). Thus, higher expression of *ITGA3* correlated with poor prognosis in ovarian cancer, especially in the high grade serous type. In addition, integrin $\alpha 3$ expression was positively correlated with laminin expression, according to IHC staining of 31 ovarian cancer patient samples (Figure 5D). By visually analyzing TCGA data with the cBio Cancer Genomics Portal (<http://cbioportal.org>)^{50,51}, we found that expression levels of laminin-related genes, including *LAMA3*, *LAMB3*, and *LAMC2*, were positively correlated with *ITGA3* expression in ovarian cancer (Figure 5E), consistent with our IHC results. Therefore, we also analyzed the correlations between patient survival and *LAMA3*, *LAMB3*, and *LAMC2* expression using the Kaplan-Meier Plotter database. Elevated *LAMA3* and *LAMC2* expression alone or in combination with high *ITGA3* expression correlated with poor prognosis. However, *LAMB3* expression was not significantly correlated with survival when analyzed alone or in combination with *ITGA3* expression (Figure 5F,G).

4 | DISCUSSION

Targeted cancer therapies are often more effective and less harmful to normal cells than traditional chemotherapy, as exemplified by PARP inhibitors and anti-angiogenesis drugs currently in clinical trials for ovarian cancer.⁵² In this study, we developed novel mAbs that specifically target ovarian cancer. We generated hybridomas that accurately target the ovarian cancer cell line, SKOV-3, and then studied the cellular effects of these mAbs. Subsequently, OV-Ab 30-7 was found to target the surface protein, integrin $\alpha 3$ (but not integrin $\beta 1$), and directly induced apoptosis in cancer cells, as evidenced by activation of caspase-3, increased cleavage of PARP, and upregulation of p53 and p21 proteins. To the best of our knowledge, this is the first study to describe an anti-integrin $\alpha 3$ mAb that directly induces cancer cell death, rather than stimulating antibody-dependent cellular cytotoxicity or complement-dependent cytotoxicity.

OV-Ab 30-7 can block the laminin-integrin interaction and inhibit downstream FAK protein phosphorylation. It is well known that activation of FAK protein by laminin-integrin $\alpha 3$ binding promotes tumor growth and metastasis.^{53,54} Previous studies have found that laminin enhanced cellular migration by binding to the integrin $\alpha 3\beta 1$ heterodimer, and blockade of this interaction by anti-laminin mAb strongly inhibited integrin $\alpha 3\beta 1$ -mediated adhesion and migration of cancer cells.^{21,55} In ovarian cancer, FAK overexpression was found in 68% of

invasive ovarian cancers and is associated with advanced tumor stage, distant metastasis and poor prognosis.⁵⁶ FAK signaling is also associated with ovarian cancer resistance to PTX.^{57,58} Treatment of taxane-resistant cell lines with FAK inhibitor can override PTX resistance by decreasing YB-1 transcription factor phosphorylation in an Akt-dependent pathway.⁵⁷ Additionally, FAK can promote cell survival by activating the phosphatidylinositol 3-kinase-AKT signaling pathway and suppressing p53-mediated apoptosis.⁵⁹ Moreover, deactivation of FAK by antibody,^{60,61} antisense oligonucleotide⁶² and siRNA⁶³ were all shown to induce apoptosis in various cancer cells. Therefore, the OV-Ab 30-7 blockade of integrin $\alpha 3$ binding to laminin, which inhibits laminin-induced FAK phosphorylation, is a well supported and likely mechanism to produce therapeutic effects in ovarian cancer.

The role of integrin $\alpha 3$ in ovarian cancer has not been conclusively demonstrated. We found that integrin $\alpha 3$ is overexpressed in ovarian cancer compared with normal ovarian tissue. Furthermore, our analyses of patient survival using online databases showed significant reductions of progression-free survival when *ITGA3* expression level was high. Not surprisingly, laminin expression was correlated with integrin $\alpha 3$ expression, and it was also correlated with poor prognosis in ovarian cancer. Due to the small sample size in our experiment, the expression profiles we found for integrin $\alpha 3$ and laminin might not accurately reflect the entire population of ovarian cancer patients. However, our findings were consistent with several other cancer types, such as breast, colon, lung, oral, pancreatic, and liver cancers.⁶⁴⁻⁷³

Ovarian cancer is the deadliest gynecological cancer, largely because it is often diagnosed at advanced stages.⁷⁴ Combination of PTX and a platinum drug is a standard first-line treatment for advanced and metastatic ovarian cancer. Although most patients respond well to this primary treatment, the majority eventually develop a recurrence.⁵ To evaluate the therapeutic potential of OV-Ab 30-7, we investigated the therapeutic effect of the antibody in a model of metastatic ovarian cancer. We treated a human ovarian cancer metastatic animal model with either PTX + CBP alone or PTX + CBP in combination with OV-Ab 30-7. Our results revealed that administration of OV-Ab 30-7 enhanced the antitumor activity of PTX + CBP. Importantly, OV-Ab 30-7 markedly prolonged the median overall survival of metastatic tumor-bearing mice without causing significant changes in body weight. Hence, OV-Ab 30-7 may potentially increase the therapeutic index of the current metastatic ovarian cancer treatment regimens, when used in combination.

Currently, there are 2 integrin-targeting mAbs that have the potential to be used as treatments for ovarian cancer. One is Volociximab, a high-affinity, chimeric antibody against human $\alpha 5\beta 1$ -integrin.⁷⁵ Volociximab inhibits survival and proliferation of endothelial cells, and it also inhibits ovarian cancer cell metastasis in vivo.⁷⁶ However, this antibody failed in a phase II clinical trial due to insufficient efficacy for preventing cancer progression and adverse effects (NCT00516841).⁷⁷ The other is Intetumumab (CNT095), which is a human monoclonal antibody against pan- αv -integrin.⁷⁸ Treatment with Intetumumab induced complete response in 1 patient with ovarian cancer in a phase

I clinical study.⁷⁹ This drug has not yet progressed to advanced ovarian cancer trials.⁸⁰ A previous study also reported a humanized mAb, ONS-M21, which could specifically recognize integrin $\alpha 3$ in gliomas and medulloblastomas without reacting to normal brain tissue.³⁰ However, to the best of our knowledge, there is currently no integrin $\alpha 3$ -targeting therapeutic antibody under development. Targeting integrin $\alpha 3$ might cause adverse effects as the protein is required for basement-membrane structures within the kidney, lung, and skin^{81,82} and it is also widely expressed in both fetal and adult epidermis.^{23,83} Despite this potential, we found that OV-Ab 30-7 did not induce normal epithelial cell apoptosis, raising the possibility that OV-Ab 30-7 induces cancer cell apoptosis due to oncogenic addiction; this idea is similar to in our previous study on the anti-EpCAM antibody, EpAb2-6.^{40,84} Nevertheless, more extensive experiments are needed to address the potential side-effects of OV-Ab 30-7. Treating the antibody by peritoneal injection might minimize off-target effects while retaining anti-cancer activity as ovarian cancer cells usually disseminate through the peritoneal cavity.⁸⁵ The epitope of OV-Ab 30-7 has not been determined. Several studies have found that mAbs may bind to a specific protein conformation or glycosylation site critical for cancer-specificity.^{86,87} As OV-Ab 30-7 inhibits laminin-induced signaling, we hypothesized that the epitope may be associated with the laminin binding domain on integrin $\alpha 3$. Additionally, we should note that because mouse antibodies are highly immunogenic in humans, OV-Ab 30-7 must be humanized prior to clinical application.

In the present study, we demonstrated that OV-Ab 30-7 recognizes integrin $\alpha 3$ and can inhibit ligand-mediated integrin-FAK signaling, while directly inducing ovarian cancer cell death. Our study introduces integrin $\alpha 3$ as a potential therapeutic target in ovarian cancer and provides a novel biologic drug candidate for this purpose.

ACKNOWLEDGMENTS

We thank the Core Facility of the Institute of Cellular and Organismic Biology (Taipei, Taiwan), National RNAi Core Facility, Academia Sinica (Taipei, Taiwan) and Academia Sinica SPF Animal Core Facility for animal study and technical support. The core facility is funded by the Academia Sinica Core Facility and Innovative Instrument Project (AS-CFII-108-103). This research was supported by Academia Sinica [AS-SUMMIT-108] and Ministry of Science and Technology [MOST-108-3114-Y-001-002], [MOST-108-2823-8-001-001], and the Program for Translational Innovation of Biopharmaceutical Development - Technology Supporting Platform Axis and [107-0210-01-19-04], Taiwan (to H.-C. Wu), and partially supported by grant [NTU-CDP-103R7837] (to K.-T. Kuo). The results published here are in part based upon data generated by the TCGA Research Network: <https://www.cancer.gov/tcga>.

DISCLOSURE

All authors have no conflicts of interest to disclose.

ORCID

Kuan-Ting Kuo  <https://orcid.org/0000-0002-3657-1652>

Han-Chung Wu  <https://orcid.org/0000-0002-5185-1169>

REFERENCES

1. Bray F, Ferlay J, Soerjomataram I, Siegel RL, Torre LA, Jemal A. Global cancer statistics 2018: GLOBOCAN estimates of incidence and mortality worldwide for 36 cancers in 185 countries. *CA Cancer J Clin*. 2018;68(6):394-424.
2. Peres LC, Cushing-Haugen KL, Köbel M, et al. Invasive epithelial ovarian cancer survival by histotype and disease stage. *J Natl Cancer Inst*. 2019;111(1):60-68.
3. Hilliard TS. The impact of mesothelin in the ovarian cancer tumor microenvironment. *Cancers (Basel)*. 2018;10(9):277.
4. Vergote I, Tropé CG, Amant F, et al. Neoadjuvant chemotherapy or primary surgery in stage IIIC or IV ovarian cancer. *N Engl J Med*. 2010;363(10):943-953.
5. Heintz A, Odicino F, Maisonneuve P, et al. Carcinoma of the ovary. FIGO 26th annual report on the results of treatment in gynecological cancer. *Int J Gynaecol Obstet*. 2006;95(Suppl 1):S161-S192.
6. Monk BJ, Coleman RL. Changing the paradigm in the treatment of platinum-sensitive recurrent ovarian cancer: from platinum doublets to nonplatinum doublets and adding antiangiogenesis compounds. *Int J Gynecol Cancer*. 2009;19(Suppl 2):S63-S67.
7. Vaughan S, Coward JI, Bast RC, et al. Rethinking ovarian cancer: recommendations for improving outcomes. *Nat Rev Cancer*. 2011;11(10):719-725.
8. Monk BJ, Choi DC, Pugmire G, Burger RA. Activity of bevacizumab (rhuMAB VEGF) in advanced refractory epithelial ovarian cancer. *Gynecol Oncol*. 2005;96(3):902-905.
9. Aghajanian C. The role of bevacizumab in ovarian cancer—an evolving story. *Gynecol Oncol*. 2006;102(2):131-133.
10. Meehan RS, Chen AP. New treatment option for ovarian cancer: PARP inhibitors. *Gynecol Oncol Res Pract*. 2016;3:3.
11. Burger RA, Enserro D, Tewari KS, et al. Final overall survival (OS) analysis of an international randomized trial evaluating bevacizumab (BEV) in the primary treatment of advanced ovarian cancer: a NRG oncology/Gynecologic Oncology Group (GOG) study. *J Clin Oncol*. 2018;36(15_suppl):5517.
12. Aghajanian C, Blank SV, Goff BA, et al. OCEANS: a randomized, double-blind, placebo-controlled phase III trial of chemotherapy with or without bevacizumab in patients with platinum-sensitive recurrent epithelial ovarian, primary peritoneal, or fallopian tube cancer. *J Clin Oncol*. 2012;30(17):2039-2045.
13. Oza AM, Cook AD, Pfisterer J, et al. Standard chemotherapy with or without bevacizumab for women with newly diagnosed ovarian cancer (ICON7): overall survival results of a phase 3 randomised trial. *Lancet Oncol*. 2015;16(8):928-936.
14. Perren TJ, Swart AM, Pfisterer J, et al. A phase 3 trial of bevacizumab in ovarian cancer. *N Engl J Med*. 2011;365(26):2484-2496.
15. Ledermann J, Harter P, Gourley C, et al. Olaparib maintenance therapy in platinum-sensitive relapsed ovarian cancer. *N Engl J Med*. 2012;366(15):1382-1392.
16. Han Y, Chen MK, Wang HL, et al. Synergism of PARP inhibitor fluzoparib (HS10160) and MET inhibitor HS10241 in breast and ovarian cancer cells. *Am J Cancer Res*. 2019;9(3):608-618.
17. Ledermann J, Harter P, Gourley C, et al. Olaparib maintenance therapy in patients with platinum-sensitive relapsed serous ovarian cancer: a preplanned retrospective analysis of outcomes by BRCA status in a randomised phase 2 trial. *Lancet Oncol*. 2014;15(8):852-861.
18. McNeish IA, Oza AM, Coleman RL, et al. Results of ARIEL2: A Phase 2 trial to prospectively identify ovarian cancer patients likely to respond to rucaparib using tumor genetic analysis. *J Clin Oncol*. 2015;33(15_suppl):5508.

19. Hynes RO. Integrins: bidirectional, allosteric signaling machines. *Cell*. 2002;110(6):673-687.
20. Kikkawa Y, Sanzen N, Fujiwara H, Sonnenberg A, Sekiguchi K. Integrin binding specificity of laminin-10/11: laminin-10/11 are recognized by alpha 3 beta 1, alpha 6 beta 1 and alpha 6 beta 4 integrins. *J Cell Sci*. 2000;113(Pt 5):869-876.
21. Kawataki T, Yamane T, Naganuma H, et al. Laminin isoforms and their integrin receptors in glioma cell migration and invasiveness: evidence for a role of alpha5-laminin(s) and alpha3beta1 integrin. *Exp Cell Res*. 2007;313(18):3819-3831.
22. Nishiuchi R, Takagi J, Hayashi M, et al. Ligand-binding specificities of laminin-binding integrins: a comprehensive survey of laminin-integrin interactions using recombinant alpha3beta1, alpha6beta1, alpha7beta1 and alpha6beta4 integrins. *Matrix Biol*. 2006;25(3):189-197.
23. Margadant C, Charafeddine RA, Sonnenberg A. Unique and redundant functions of integrins in the epidermis. *FASEB J*. 2010;24(11):4133-4152.
24. Hertle MD, Adams JC, Watt FM. Integrin expression during human epidermal development in vivo and in vitro. *Development*. 1991;112(1):193-206.
25. DiPersio CM, Hovalva-Dilke KM, Jaenisch R, Kreidberg JA, Hynes RO. alpha3beta1 Integrin is required for normal development of the epidermal basement membrane. *J Cell Biol*. 1997;137(3):729-742.
26. Kreidberg JA, Donovan MJ, Goldstein SL, et al. Alpha 3 beta 1 integrin has a crucial role in kidney and lung organogenesis. *Development*. 1996;122(11):3537-3547.
27. Anton ES, Kreidberg JA, Rakic P. Distinct functions of alpha3 and alpha(v) integrin receptors in neuronal migration and laminar organization of the cerebral cortex. *Neuron*. 1999;22(2):277-289.
28. Xiao W, Yao N, Peng L, Liu R, Lam KS. Near-infrared optical imaging in glioblastoma xenograft with ligand-targeting alpha 3 integrin. *Eur J Nucl Med Mol Imaging*. 2009;36(1):94-103.
29. Aina OH, Marik J, Gandour-Edwards R, Lam KS. Near-infrared optical imaging of ovarian cancer xenografts with novel alpha 3-integrin binding peptide "OA02". *Mol Imaging*. 2005;4(4):439-447.
30. Kishima H, Shimizu K, Tamura K, et al. Monoclonal antibody ONS-M21 recognizes integrin alpha3 in gliomas and medulloblastomas. *Br J Cancer*. 1999;79(2):333-339.
31. Gourley C, Paige AJ, Taylor KJ, et al. WWOX gene expression abolishes ovarian cancer tumorigenicity in vivo and decreases attachment to fibronectin via integrin alpha3. *Cancer Res*. 2009;69(11):4835-4842.
32. Baldwin LA, Hoff JT, Lefringhouse J, et al. CD151-alpha3beta1 integrin complexes suppress ovarian tumor growth by repressing slug-mediated EMT and canonical Wnt signaling. *Oncotarget*. 2014;5(23):12203-12217.
33. Suzuki N, Higashiguchi A, Hasegawa Y, et al. Loss of integrin alpha3 expression associated with acquisition of invasive potential by ovarian clear cell adenocarcinoma cells. *Hum Cell*. 2005;18(3):147-155.
34. Kroschinsky F, Stölzel F, von Bonin S, et al. New drugs, new toxicities: severe side effects of modern targeted and immunotherapy of cancer and their management. *Crit Care*. 2017;21(1):89.
35. Lee TY, Wu HC, Tseng YL, Lin CT. A novel peptide specifically binding to nasopharyngeal carcinoma for targeted drug delivery. *Cancer Res*. 2004;64(21):8002-8008.
36. Chu Y-W, Yang P-C, Yang S-C, et al. Selection of invasive and metastatic subpopulations from a human lung adenocarcinoma cell line. *Am J Respir Cell Mol Biol*. 1997;17(3):353-360.
37. Tung KH, Lin CW, Kuo CC, et al. CHC promotes tumor growth and angiogenesis through regulation of HIF-1alpha and VEGF signaling. *Cancer Lett*. 2013;331(1):58-67.
38. Lu R-M, Hwang Y-C, Liu I-J, et al. Development of therapeutic antibodies for the treatment of diseases. *J Biomed Sci*. 2020;27(1):1.
39. Liu IJ, Chiu CY, Chen YC, Wu HC. Molecular mimicry of human endothelial cell antigen by autoantibodies to nonstructural protein 1 of dengue virus. *J Biol Chem*. 2011;286(11):9726-9736.
40. Liao M-Y, Lai J-K, Kuo M-P, et al. An anti-EpCAM antibody EpAb2-6 for the treatment of colon cancer. *Oncotarget*. 2015;6(28):24947-24968.
41. Fujiwara K, Shintani D, Nishikawa T. Clear-cell carcinoma of the ovary. *Ann Oncol*. 2016;27(Suppl 1):i50-i52.
42. Yu L, Wang Y, Yao Y, et al. Eradication of growth of HER2-positive ovarian cancer with trastuzumab-DM1, an antibody-cytotoxic drug conjugate in mouse xenograft model. *Int J Gynecol Cancer*. 2014;24(7):1158-1164.
43. Lanitis E, Poussin M, Hagemann IS, et al. Redirected antitumor activity of primary human lymphocytes transduced with a fully human anti-mesothelin chimeric receptor. *Mol Ther*. 2012;20(3):633-643.
44. Shen Y-A, Liu C-S, Chang Y-H, et al. Subtype-specific binding peptides enhance the therapeutic efficacy of nanomedicine in the treatment of ovarian cancer. *Cancer Lett*. 2015;360(1):39-47.
45. Shield K, Riley C, Quinn MA, Rice GE, Ackland ML, Ahmed N. Alpha2beta1 integrin affects metastatic potential of ovarian carcinoma spheroids by supporting disaggregation and proteolysis. *J Carcinog*. 2007;6:11.
46. Casey RC, Burleson KM, Skubitz KM, et al. Beta 1-integrins regulate the formation and adhesion of ovarian carcinoma multicellular spheroids. *Am J Pathol*. 2001;159(6):2071-2080.
47. Kikkawa Y, Sanzen N, Sekiguchi K. Isolation and characterization of laminin-10/11 secreted by human lung carcinoma cells. laminin-10/11 mediates cell adhesion through integrin alpha3 beta1. *J Biol Chem*. 1998;273(25):15854-15859.
48. Delwel GO, de Melker AA, Hogervorst F, et al. Distinct and overlapping ligand specificities of the alpha 3A beta 1 and alpha 6A beta 1 integrins: recognition of laminin isoforms. *Mol Biol Cell*. 1994;5(2):203-215.
49. Chiang Y-C, Chen C-A, Chiang C-J, et al. Trends in incidence and survival outcome of epithelial ovarian cancer: 30-year national population-based registry in Taiwan. *J Gynecol Oncol*. 2013;24(4):342-351.
50. Cerami E, Gao J, Dogrusoz U, et al. The cBio cancer genomics portal: an open platform for exploring multidimensional cancer genomics data. *Cancer Discov*. 2012;2(5):401-404.
51. Gao J, Aksoy BA, Dogrusoz U, et al. Integrative analysis of complex cancer genomics and clinical profiles using the cBioPortal. *Sci Signal*. 2013;6(269):p1.
52. Cortez AJ, Tudrej P, Kujawa KA, Lisowska KM. Advances in ovarian cancer therapy. *Cancer Chemother Pharmacol*. 2018;81(1):17-38.
53. Choma DP, Milano V, Pumiglia KM, DiPersio CM. Integrin alpha3beta1-dependent activation of FAK/Src regulates Rac1-mediated keratinocyte polarization on laminin-5. *J Invest Dermatol*. 2007;127(1):31-40.
54. Mitra SK, Schlaepfer DD. Integrin-regulated FAK-Src signaling in normal and cancer cells. *Curr Opin Cell Biol*. 2006;18(5):516-523.
55. Wondimu Z, Omrani S, Ishikawa T, et al. A novel monoclonal antibody to human laminin alpha5 chain strongly inhibits integrin-mediated cell adhesion and migration on laminins 511 and 521. *PLoS One*. 2013;8(1):e53648.
56. Sood AK, Coffin JE, Schneider GB, et al. Biological significance of focal adhesion kinase in ovarian cancer: role in migration and invasion. *Am J Pathol*. 2004;165(4):1087-1095.
57. Kang YU, Hu W, Ivan C, et al. Role of focal adhesion kinase in regulating YB-1-mediated paclitaxel resistance in ovarian cancer. *J Natl Cancer Inst*. 2013;105(19):1485-1495.
58. McGrail DJ, Khambhati NN, Qi MX, et al. Alterations in ovarian cancer cell adhesion drive taxol resistance by increasing microtubule dynamics in a FAK-dependent manner. *Sci Rep*. 2015;5:9529.
59. Schlaepfer DD, Mitra SK, Ilic D. Control of motile and invasive cell phenotypes by focal adhesion kinase. *Biochim Biophys Acta*. 2004;1692(2-3):77-102.

60. Hungerford JE, Compton MT, Matter ML, Hoffstrom BG, Otey CA. Inhibition of pp125FAK in cultured fibroblasts results in apoptosis. *J Cell Biol.* 1996;135(5):1383-1390.
61. Liu XJ, Yang L, Wu HB, Qiang O, Huang MH, Wang YP. Apoptosis of rat hepatic stellate cells induced by anti-focal adhesion kinase antibody. *World J Gastroenterol.* 2002;8(4):734-738.
62. Xu LH, Owens LV, Sturge GC, et al. Attenuation of the expression of the focal adhesion kinase induces apoptosis in tumor cells. *Cell Growth Differ.* 1996;7(4):413-418.
63. Duxbury MS, Ito H, Zinner MJ, Ashley SW, Whang EE. Focal adhesion kinase gene silencing promotes anoikis and suppresses metastasis of human pancreatic adenocarcinoma cells. *Surgery.* 2004;135(5):555-562.
64. Giannelli G, Fransvea E, Marinosci F, et al. Transforming growth factor-beta1 triggers hepatocellular carcinoma invasiveness via alpha-3beta1 integrin. *Am J Pathol.* 2002;161(1):183-193.
65. Zhu G-H, Huang C, Qiu Z-J, et al. Expression and prognostic significance of CD151, c-Met, and integrin alpha3/alpha6 in pancreatic ductal adenocarcinoma. *Dig Dis Sci.* 2011;56(4):1090-1098.
66. Chen WL, Wang XK, Wu W. Identification of ITGA3 as an Oncogene in Human Tongue Cancer via Integrated Bioinformatics Analysis. *Curr Med Sci.* 2018;38(4):714-720.
67. Ramovs V, Te Molder L, Sonnenberg A. The opposing roles of laminin-binding integrins in cancer. *Matrix Biol.* 2017;57-58:213-243.
68. Ghosh S, Koblinski J, Johnson J, et al. Urinary-type plasminogen activator receptor/alpha 3 beta 1 integrin signaling, altered gene expression, and oral tumor progression. *Mol Cancer Res.* 2010;8(2):145-158.
69. Yoshimasu T, Sakurai T, Oura S, et al. Increased expression of integrin alpha3beta1 in highly brain metastatic subclone of a human non-small cell lung cancer cell line. *Cancer Sci.* 2004;95(2):142-148.
70. Zhou B, Gibson-Corley KN, Herndon ME, et al. Integrin alpha-3beta1 can function to promote spontaneous metastasis and lung colonization of invasive breast carcinoma. *Mol Cancer Res.* 2014;12(1):143-154.
71. Lenander C, Habermann JK, Ost A, et al. Laminin-5 gamma 2 chain expression correlates with unfavorable prognosis in colon carcinomas. *Anal Cell Pathol.* 2001;22(4):201-209.
72. Masuda R, Kijima H, Imamura N, et al. Laminin-5gamma2 chain expression is associated with tumor cell invasiveness and prognosis of lung squamous cell carcinoma. *Biomed Res.* 2012;33(5):309-317.
73. Lee J, Lee J, Choi C, Kim JH. Blockade of integrin alpha3 attenuates human pancreatic cancer via inhibition of EGFR signalling. *Sci Rep.* 2019;9(1):2793.
74. Torre LA, Trabert B, DeSantis CE, et al. Ovarian cancer statistics, 2018. *CA Cancer J Clin.* 2018;68(4):284-296.
75. Ramakrishnan V, Bhaskar V, Law DA, et al. Preclinical evaluation of an anti-alpha5beta1 integrin antibody as a novel anti-angiogenic agent. *J Exp Ther Oncol.* 2006;5(4):273-286.
76. Mitra AK, Sawada K, Tiwari P, Mui K, Gwin K, Lengyel E. Ligand-independent activation of c-Met by fibronectin and alpha(5)beta(1)-integrin regulates ovarian cancer invasion and metastasis. *Oncogene.* 2011;30(13):1566-1576.
77. Bell-McGuinn KM, Matthews CM, Ho SN, et al. A phase II, single-arm study of the anti-alpha5beta1 integrin antibody volociximab as monotherapy in patients with platinum-resistant advanced epithelial ovarian or primary peritoneal cancer. *Gynecol Oncol.* 2011;121(2):273-279.
78. O'Day S, Pavlick A, Loquai C, et al. A randomised, phase II study of intetumumab, an anti-alphav-integrin mAb, alone and with dacarbazine in stage IV melanoma. *Br J Cancer.* 2011;105(3):346-352.
79. Mullamitha SA, Ton NC, Parker GJ, et al. Phase I evaluation of a fully human anti-alphav integrin monoclonal antibody (CNTO 95) in patients with advanced solid tumors. *Clin Cancer Res.* 2007;13(7):2128-2135.
80. Moffitt L, Karimnia N, Stephens A, Bilandzic M. Therapeutic targeting of collective invasion in ovarian cancer. *Int J Mol Sci.* 2019;20(6):1466.
81. Has C, Sparta G, Kiritsi D, et al. Integrin alpha3 mutations with kidney, lung, and skin disease. *N Engl J Med.* 2012;366(16):1508-1514.
82. de Melker AA, Sterk LM, Delwel GO, et al. The A and B variants of the alpha 3 integrin subunit: tissue distribution and functional characterization. *Lab Invest.* 1997;76(4):547-563.
83. Bartolazzi A, Cerboni C, Full C, et al. V1a-3 distribution in normal and neoplastic non-lymphoid human tissues. *Pathol Res Pract.* 1993;189(4):387-393.
84. Liang K-H, Tso H-C, Hung S-H, et al. Extracellular domain of EpCAM enhances tumor progression through EGFR signaling in colon cancer cells. *Cancer Lett.* 2018;433:165-175.
85. Lengyel E. Ovarian cancer development and metastasis. *Am J Pathol.* 2010;177(3):1053-1064.
86. Kato Y, Kaneko MK. A cancer-specific monoclonal antibody recognizes the aberrantly glycosylated podoplanin. *Sci Rep.* 2014;4:5924.
87. Hosen N, Matsunaga Y, Hasegawa K, et al. The activated conformation of integrin beta7 is a novel multiple myeloma-specific target for CAR T cell therapy. *Nat Med.* 2017;23(12):1436-1443.

SUPPORTING INFORMATION

Additional supporting information may be found online in the Supporting Information section.

How to cite this article: Ke F-Y, Chen W-Y, Lin M-C, Hwang Y-C, Kuo K-T, Wu H-C. Novel monoclonal antibody against integrin α 3 shows therapeutic potential for ovarian cancer. *Cancer Sci.* 2020;111:3478-3492. <https://doi.org/10.1111/cas.14566>